BULETINUL INSTITUTULUI POLITEHNIC DIN IAŞI
Publicat de
Universitatea Tehnică „Gheorghe Asachi" din Iaşi
Volumul 63 (67), Numărul 2, 2017
Secţia
ELECTROTEHNICĂ. ENERGETICĂ. ELECTRONICĂ

STUDY OF ELECTROENCEPHALOGRAPHIC CHANNELS COUPLING IN MULTIPLE DATABASE ANALYSIS

BY

ALEXANDRU PĂSĂRICĂ[1,2,*], OANA DIANA EVA[1,2] and DANIELA TĂRNICERIU[1]

[1]Technical University "Gheorghe Asachi" of Iaşi,
Faculty of Electronics, Telecommunications and Information Technology,
[2] Institute of Computer Science, Romanian Academy

Received: April 28, 2017
Accepted for publication: May 30, 2017

Abstract. Encephalographic (EEG) signal analysis of motor imagery tasks can be used to implement human machine interaction applications. This implies a good understanding of the brain activity during cerebral events. The use of the partial directed coherence (PDC) method to analyse multiple EEG signal databases can determine coupling levels between channels in order to assess EEG data processing and data acquisition for these types of applications. This is necessary for reducing the processing time and responsiveness of systems developed for human computer interaction.

Key words: brain-computer interface; correlation analysis; partial directed coherence; signal processing.

1. Introduction

The brain activity relies on high level sensory and cognitive functions between different brain areas. The analysis of electroencephalographic (EEG) signals is used to identify these connections in order to develop further applications that can allow a better understanding of the human brain (Pfurtscheller *et al*., 2000). In recent years, one type of application consists in

[*]Corresponding author: *e-mail*: alexpasarica@gmail.com

implementation of an interface for human computer interaction, named brain computer interface (BCI). This device is designed in order to enable the subject to communicate without using the peripheral nervous system, which is involved in the conduction of impulses from the brain to the muscles and also provides biofeedback from sensory receptors in sensing organs or neuro-motor activity (Petti *et al*., 2016). The complexity of these devices often leads to a high processing time of the recordings acquired, so that it is necessary to determine the optimal setup to be used in terms of number of electrodes and positioning. For brain computer interface (BCI) applications the number of EEG channels analysed is usually between 8 and 16 (Pichiorri *et al*., 2015).

The paper presents the analysis of coupling between channel pairs for EEG recordings taken during motor imagery tasks, movement or resting periods. The coupling level is determined using the partial directed coherence (PDC) method which is based on the Granger causality for the frequency domain (Friston *et al*., 2016). For a more in depth analysis, we divide the EEG frequency domain of 0,...,30 Hz into four separate frequency bands based on the EEG rhythms: Delta, Theta, Alpha, and Beta. This method allows us to establish different features for motor imagery tasks and resting period recordings. The PDC method is used to analyse the EEG signals taking into account the frequency domain 0,...,30 Hz as a whole. Some reference papers presenting the EEG analysis using the PDC method are Lee *et al*., 2016, Omidvarnia *et al*., 2013 and Liang *et al*., 2016.

2. Databases and Methods

A. *Databases*

The first database analysed is the EEG Motor Movement/Imagery Dataset publicly available from the Physionet.org platform, referred to as DB1 (Goldberger *et al*., 2000). This contains over 1,500 EEG recordings, from 108 different subjects. These recordings present 64 EEG channels acquired and are 1 to 2 minutes long, with a sampling frequency of 160 Hz. The system used to acquire these recordings is the BCI 2000 device (Link 1) (Shalk *et al*., 2004).

The database is structured in 14 sub-recordings for each of the 108 subjects, defined as follows:

1. Baseline EEG signals when the eyes are open.
2. Baseline EEG signals when the eyes are closed.
3. Movement of opening and closing the left or right fist.
4. Imagining of opening and closing the left or right fist.
5. Movement of opening and closing both fists and feet.
6. Imagining of opening and closing both fists and feet.
7. Movement of opening and closing the left or right fist.
8. Imagining of opening and closing the left or right fist.
9. Movement of opening and closing both fists and feet.
10. Imagining of opening and closing both fists and feet.

11. Movement of opening and closing the left or right fist.
12. Imagining of opening and closing the left or right fist.
13. Movement of opening and closing both fists and feet.
14. Imagining of opening and closing both fists and feet.

We select for this analysis the recordings that correspond to the movement of opening and closing the left or right fist (3.7 and 11) and the recordings for the movement imagination of opening and closing the left or right fist (4.8 and 12) (324 movement recordings and 323 imaginary movement recordings - one recording was missing for one subject).

The second database analysed, referred to as DB2, is represented by the BCI Competition IV database from the Technical University of Berlin (Link 2), (Blankertz *et al.*, 2007). This contains 10 EEG recordings, 59 channels acquired, at a sampling frequency of 1,000 Hz with a resolution of 16 bits. The device used to acquire the data was the BCI2000.

The signals were bandpass filtered between 0.05 and 200 Hz. Each recording consists of motor imagery cues for two classes: imagery movement of the left or right hand, and resting period recordings. These events are marked for each recording and, in order to perform our analysis, we divide the recordings based on these markers. Events are represented by 4 s periods corresponding to the motor imagery task and 4 s periods of resting between consecutive tasks. We obtained 994 short time recordings for the left hand (497 motor imagery tasks of the left hand with 497 resting phases between tasks) and 998 short recordings for the right hand (499 motor imagery tasks of the right hand with 499 resting phases between tasks). The database also contains recordings of motor imagery tasks of the foot, but these were not selected for this analysis as we desired that both databases have similar types of recordings (*e.g.* motor imagery of hands).

The EEG channels we have analysed in order to obtain the coupling level were (Niedermeyer *et al.*, 2005): FC3, FC4, C3, C4, Cz, CP3, CP4, F1, F2, Fz, Pz.

B. *Partial directed coherence method*

The method implemented for this analysis is the partial directed coherence (PDC) (Baccala & Sameshima, 2001) which has been adapted for this application by dividing the EEG frequency interval 0,...,30 Hz into frequency bands that correspond to different EEG rhythms. The first frequency band is between 0,...,8 Hz and is specific to Delta, Theta and Alpha1 rhythm, the second frequency band is between 8,...,12 Hz and corresponds to Alpha2 rhythm, the third frequency band is between 12,...,18 Hz and is specific to the Beta1 rhythm, and the last band that is between 18,...,30 Hz for the Beta2 rhythm (Tsoneva *et al.*, 2011). The paper performs a comparison of coupling between EEG channels for both motor imagery and movement recordings. It is performed to determine the possibility of analysing certain channel pairs in order to implement BCI application for future development of communication devices between human and computer.

The PDC method is implemented by defining the multivariate autoregressive model (MVAR) of the analysed EEG channels; in our case we have experimentally selected 11 channels and considered studies of similar applications in the literature. The MVAR model of order $p = 2$ is defined by the formula (Adochiei *et al*., 2013a):

$$\begin{bmatrix} x_1(n) \\ \vdots \\ x_N(n) \end{bmatrix} = \sum_{r=1}^{p} A_r \begin{bmatrix} x_1(n-r) \\ \vdots \\ x_N(n-r) \end{bmatrix} + \begin{bmatrix} w_1(n) \\ \vdots \\ w_N(n) \end{bmatrix}, \quad (1)$$

where: $w(n)$ is the covariance matrix, A_r (Eq. 2) is the matrix that contains the $a_{ij}(r)$ elements that represent the linear interaction effect of $x_j(n\text{-}r)$ over $x_i(n)$:

$$A_r = \begin{bmatrix} a_{11}(r) & a_{12}(r) & \cdots & \cdots & a_{1N}(r) \\ \vdots & \vdots\ \vdots & \vdots & & \vdots \\ \vdots & \vdots\ \vdots & a_{ij}(r) & & \vdots \\ \vdots & \vdots\ \vdots & \vdots & & \vdots \\ a_{N1}(r) & \cdots & \cdots & \cdots & a_{NN}(r) \end{bmatrix}. \quad (2)$$

The influence between EEG channels is determined based on the correlation indicator value computed using (Baccala *et al*., 2007):

$$\pi_{ij}(n) = \frac{A_{ij}(n,f)}{\sqrt{a_j^H(n,f)\, a_j(n,f)}}, \quad (3)$$

where: $\pi_{ij}(n)$ is the correlation parameter, H the Hermitian transpose, $A_{ij}(n,f)$ – the Fourier transform of $A_r(n)$ with the elements $a_{ij}(n,f)$, n – the number of the analysed windows and f – the variable of the frequency bands specified before. The correlation indicator value is between [0;1], meaning that values closer to 0 represent a low level of coupling, whereas values closer to 1 represent a higher level of coupling (Adochiei *et al*., 2013b).

For this analysis we use a sliding Hanning window (Podder *et al*., 2014) with $N = 500$ samples length and an overlap of 125 samples defined by:

$$w(n) = \frac{1}{2} \times \left(1 - \cos\frac{2\pi x(n)}{N}\right); \quad 0 \le n \le N, \quad (4)$$

where: $w(n)$ is the window value for sample n, $x(n)$ – the time signal value for sample n, in this case the EEG signal, and N – the window length.

The window overlap is necessary in order to prevent information loss at the beginning and ending of the window interval due to the fact that these samples are situated towards the zero value, as presented in Fig. 1. This method also reduces the generation of side lobes, which is suitable for frequency selective applications (Samdin *et al*., 2014).

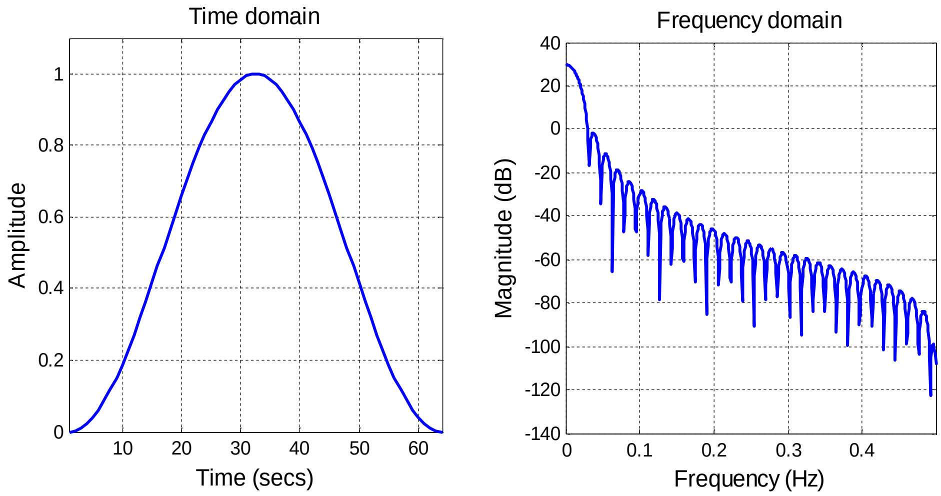

Fig. 1 – Hanning window time and frequency domain representation.

We obtain the mean PDC correlation indicator values for all 55 pairs of channels, for all recordings analysed from both databases, as presented in Table 1.

Table 1
EEG Channel Pairs Analysed

C3-C4	C4-F2	CP4-Pz	FC3-CP4	FC4-Cz
C3-CP3	C4-Fz	Cz-C4	FC3-Cz	FC4-F1
C3-CP4	C4-Pz	Cz-CP3	FC3-FC4	FC4-F2
C3-Cz	CP3-CP4	Cz-CP4	FC3-F1	FC4-Fz
C3-F1	CP3-F1	Cz-F1	FC3-F2	FC4-Pz
C3-F2	CP3-F2	Cz-F2	FC3-Fz	F1-F2
C3-Fz	CP3-Fz	Cz-Fz	FC3-Pz	F1-Fz
C3-Pz	CP3-Pz	Cz-Pz	FC4-C3	F1-Pz
C4-CP3	CP4-F1	FC3-C3	FC4-C4	F2-Fz
C4-CP4	CP4-F2	FC3-C4	FC4-CP3	F2-Pz
C4-F1	CP4-Fz	FC3-CP3	FC4-CP4	Fz-Pz

3. Experimental Results

The PDC based method analysis results were processed in order to determine the channel pairs that offer the most insight towards understanding motor imagery coupling between channels and between different areas of the brain. The results presented in Tables 2,...,6 represent the mean PDC indicator values and the standard deviation obtained for channel pairs C3-Pz, C4-Pz, F1-F2, FC3-Fz, FC4-Fz and Fz-Pz.

For the pairs C3-Pz/C4-Pz and FC3-Fz/FC4-Fz that have bilateral electrodes situated on the two hemispheres of the brain (the left and right hemispheres), we can observe high correlation values. Electrodes C3 and FC3 are located on the left brain hemisphere in the central zone, whereas electrodes C4 and FC4 are located similarly in the central zone, but on the right hemisphere. This indicates that both brain hemispheres are involved in the process of motor imagery.

A noteworthy difference between the two analysed databases can be observed between the motor imagery results, presented in Table 2 for DB1 and in Tables 4 and 5 for DB2. The difference consists in the values obtained for the direct and indirect influence between channels. DB 2 which contains short term recordings of brain activity during motor imagery tasks presents similar PDC indicator values for direct and indirect influences. Whereas DB1, which contains recordings of both motor imagery tasks and resting periods, and are longer in length overall, presents a definite difference between the values obtained for direct and indirect influences.

The observed difference between databases in terms of direct and indirect influences can only lead to the conclusion that resting periods influence the overall correlation parameter value by lowering it. The only channel pair that had similar values for both direct and indirect influences for both database is F1-F2, which considers data acquired from electrodes situated on different brain hemispheres (F1 on the left hemisphere and F2 on the right hemisphere) in the frontal area of the brain (Xu *et al.*, 2009). Nevertheless, even for this channel pair, we can observe that the correlation parameter value for DB1 is approximately 0.25 as opposed to DB2 which has a higher value of approximately 0.3, caused by the same difference in the data acquisition process mentioned before.

Table 2

PDC Correlation Indicator Mean Values for Motor Imagery (DB1)

Ch. pair	Frequency band 0-8 Hz				Frequency band 8-12 Hz				Frequency band 12-18 Hz				Frequency band 18-30 Hz			
	Med →	Std →	Med ←	Std ←	Med →	Std →	Med ←	Std ←	Med →	Std →	Med ←	Std ←	Med →	Std →	Med ←	Std ←
C3-Pz	0.236	0.068	0.182	0.074	0.236	0.064	0.182	0.071	0.236	0.061	0.182	0.059	0.263	0.074	0.263	0.058
C4-Pz	0.242	0.063	0.172	0.068	0.242	0.059	0.172	0.062	0.242	0.057	0.172	0.043	0.272	0.041	0.197	0.048
F1-F2	0.241	0.039	0.260	0.047	0.241	0.033	0.265	0.036	0.244	0.024	0.230	0.029	0.259	0.033	0.321	0.028
FC3-Fz	0.327	0.028	0.137	0.033	0.328	0.022	0.137	0.033	0.309	0.028	0.128	0.041	0.341	0.033	0.141	0.027
FC4-Fz	0.309	0.047	0.128	0.027	0.310	0.041	0.128	0.022	0.307	0.027	0.132	0.028	0.325	0.027	0.132	0.033
Fz-Pz	0.286	0.025	0.135	0.039	0.306	0.031	0.135	0.040	0.298	0.037	0.137	0.031	0.291	0.034	0.109	0.029

Table 3

PDC Correlation Indicator Mean Values for Movement Recordings (DB1)

Ch. pair	Frequency band 0-8 Hz				Frequency band 8-12 Hz				Frequency band 12-18 Hz				Frequency band 18-30 Hz			
	Med →	Std →	Med ←	Std ←	Med →	Std →	Med ←	Std ←	Med →	Std →	Med ←	Std ←	Med →	Std →	Med ←	Std ←
C3-Pz	0.238	0.068	0.178	0.024	0.239	0.034	0.178	0.041	0.245	0.021	0.120	0.029	0.263	0.024	0.198	0.028
C4-Pz	0.237	0.061	0.116	0.061	0.244	0.029	0.172	0.032	0.244	0.037	0.172	0.043	0.272	0.041	0.195	0.033
F1-F2	0.153	0.039	0.189	0.047	0.260	0.033	0.230	0.036	0.260	0.044	0.230	0.040	0.321	0.023	0.281	0.028
FC3-Fz	0.327	0.018	0.137	0.043	0.328	0.042	0.137	0.023	0.309	0.038	0.128	0.041	0.341	0.033	0.141	0.027
FC4-Fz	0.331	0.025	0.142	0.037	0.331	0.045	0.142	0.027	0.331	0.027	0.142	0.038	0.345	0.024	0.147	0.023
Fz-Pz	0.301	0.023	0.136	0.031	0.300	0.021	0.136	0.020	0.300	0.030	0.136	0.031	0.315	0.034	0.150	0.031

Table 4

PDC Correlation Indicator Mean Values for Motor Imagery Task of the Right Hand (DB2)

Ch. pair	Frequency band 0-8 Hz				Frequency band 8-12 Hz				Frequency band 12-18 Hz				Frequency band 18-30 Hz			
	Med →	Std →	Med ←	Std ←	Med →	Std →	Med ←	Std ←	Med →	Std →	Med ←	Std ←	Med →	Std →	Med ←	Std ←
C3-Pz	0.294	0.041	0.311	0.049	0.290	0.045	0.306	0.050	0.289	0.043	0.307	0.050	0.297	0.042	0.333	0.064
C4-Pz	0.298	0.041	0.320	0.048	0.291	0.042	0.314	0.052	0.295	0.040	0.312	0.050	0.294	0.039	0.343	0.065
F1-F2	0.305	0.061	0.311	0.053	0.304	0.056	0.310	0.068	0.304	0.057	0.309	0.071	0.313	0.059	0.323	0.076
FC3-Fz	0.299	0.042	0.303	0.041	0.296	0.041	0.296	0.051	0.296	0.042	0.297	0.051	0.315	0.049	0.300	0.051
FC4-Fz	0.297	0.045	0.295	0.041	0.289	0.052	0.296	0.047	0.289	0.050	0.294	0.048	0.309	0.056	0.306	0.051
Fz-Pz	0.297	0.043	0.341	0.076	0.288	0.054	0.337	0.071	0.288	0.054	0.336	0.071	0.304	0.057	0.346	0.077

Table 5

PDC Correlation Indicator Mean Values for Motor Imagery Task of the Left Hand (DB2)

Ch. pair	Frequency band 0-8 Hz				Frequency band 8-12 Hz				Frequency band 12-18 Hz				Frequency band 18-30 Hz			
	Med →	Std →	Med ←	Std ←	Med →	Std →	Med ←	Std ←	Med →	Std →	Med ←	Std ←	Med →	Std →	Med ←	Std ←
C3-Pz	0.292	0.044	0.305	0.053	0.296	0.044	0.308	0.052	0.293	0.046	0.307	0.051	0.296	0.047	0.333	0.065
C4-Pz	0.295	0.045	0.313	0.048	0.295	0.044	0.312	0.048	0.294	0.044	0.314	0.049	0.303	0.044	0.337	0.064
F1-F2	0.300	0.052	0.306	0.060	0.301	0.050	0.308	0.061	0.303	0.049	0.306	0.062	0.312	0.053	0.318	0.069
FC3-Fz	0.298	0.046	0.294	0.053	0.296	0.044	0.295	0.053	0.296	0.045	0.292	0.054	0.316	0.052	0.301	0.055
FC4-Fz	0.291	0.066	0.294	0.048	0.289	0.064	0.295	0.049	0.290	0.063	0.295	0.048	0.310	0.064	0.302	0.047
Fz-Pz	0.287	0.063	0.332	0.069	0.285	0.061	0.332	0.069	0.288	0.062	0.333	0.069	0.307	0.063	0.341	0.078

Table 6

PDC Correlation Indicator Mean Values for Rest Activity (DB2)

Ch. pair	Frequency band 0-8 Hz				Frequency band 8-12 Hz				Frequency band 12-18 Hz				Frequency band 18-30 Hz			
	Med →	Std →	Med ←	Std ←	Med →	Std →	Med ←	Std ←	Med →	Std →	Med ←	Std ←	Med →	Std →	Med ←	Std ←
C3-Pz	0.160	0.051	0.175	0.051	0.162	0.053	0.162	0.052	0.164	0.053	0.163	0.053	0.169	0.048	0.168	0.052
C4-Pz	0.171	0.052	0.171	0.049	0.172	0.054	0.163	0.053	0.170	0.054	0.162	0.054	0.175	0.051	0.168	0.050
F1-F2	0.177	0.052	0.166	0.049	0.179	0.051	0.173	0.051	0.179	0.051	0.172	0.050	0.183	0.048	0.179	0.049
FC3-Fz	0.185	0.050	0.165	0.047	0.178	0.051	0.162	0.049	0.179	0.051	0.162	0.051	0.185	0.050	0.175	0.051
FC4-Fz	0.178	0.046	0.154	0.047	0.183	0.048	0.151	0.049	0.183	0.049	0.152	0.051	0.190	0.047	0.164	0.050
Fz-Pz	0.139	0.050	0.173	0.052	0.139	0.052	0.163	0.054	0.139	0.052	0.164	0.055	0.153	0.051	0.166	0.054

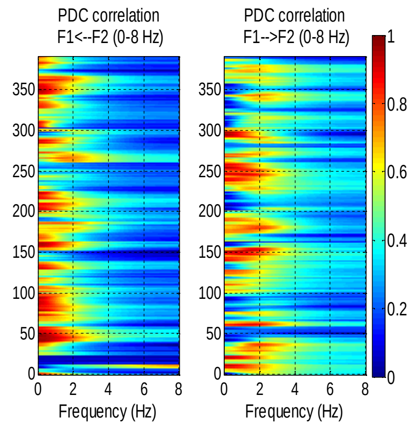

Fig. 2. a) PDC correlation for motor imagery, channel pair F1-F2, 0-8 Hz (Rec003 DB1).

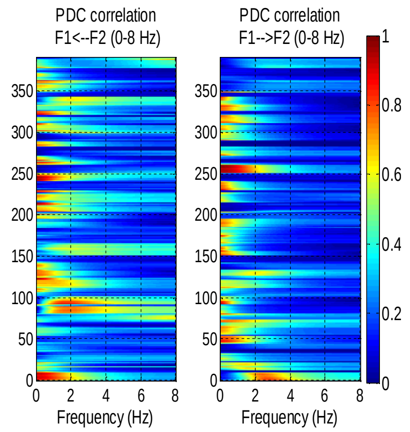

Fig. 2. b) PDC correlation for movement recordings, channel pair F1-F2, 0-8 Hz (Rec011 DB1).

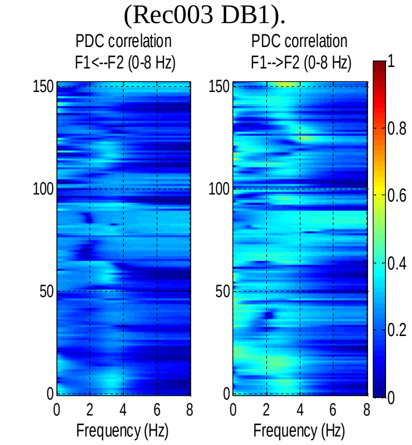

Fig. 2. c) PDC correlation for motor imagery of the left hand, channel pair F1-F2, 0-8 Hz (Rec004 DB2).

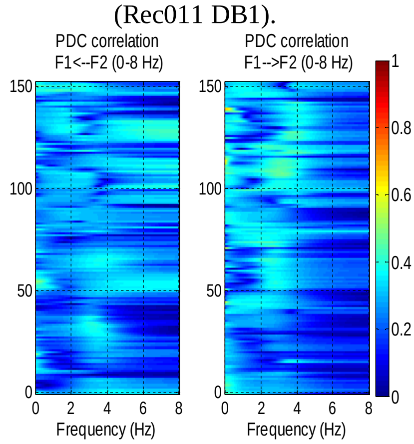

Fig. 2. d) PDC correlation for motor imagery of the right hand, channel pair F1-F2, 0-8 Hz (Rec702 DB2).

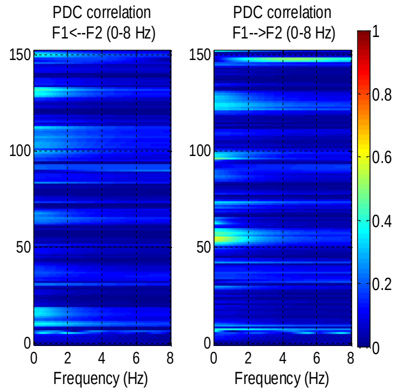

Fig. 2. e) PDC for rest recordings, pair F1-F2, 0-8 Hz (Rec014 DB2).

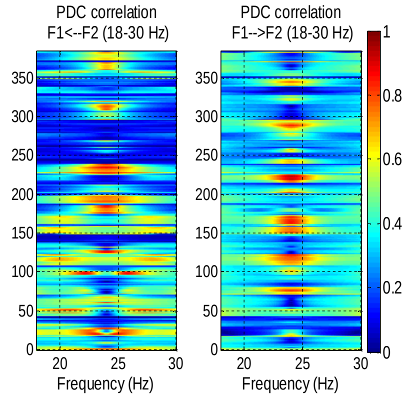

Fig. 2. f) PDC for motor imagery, F1-F2, 18-30 Hz (Rec003 DB1).

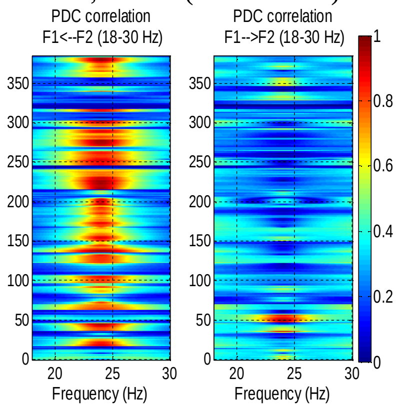

Fig. 2. g) PDC for movement recordings, pair F1-F2, 18-30 Hz (Rec011 DB1).

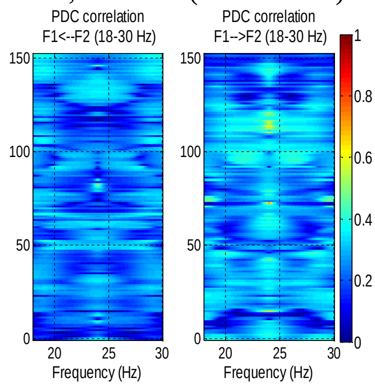

Fig. 2. h) PDC for motor imagery of the left hand, pair F1-F2, 18-30 Hz (Rec004 DB2).

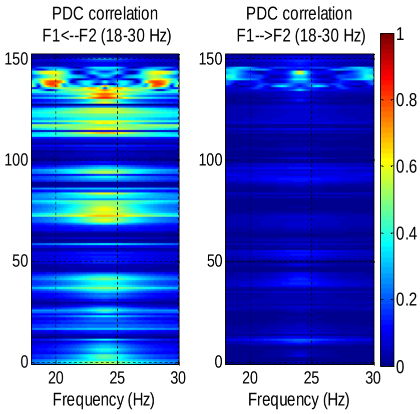

Fig. 2. i) PDC for motor imagery of the right hand, F1-F2, 18-30 Hz (Rec702 DB2).

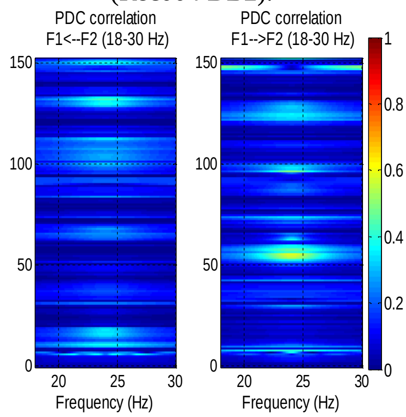

Fig. 2. j) PDC for rest recordings, F1-F2, 18-30 Hz (Rec014 DB2).

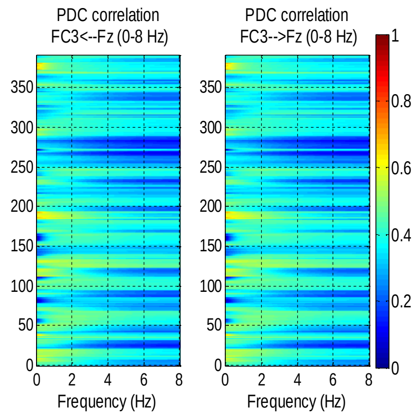

Fig. 3. a) PDC for motor imagery, FC3-Fz, 0-8 Hz (Rec003 DB1).

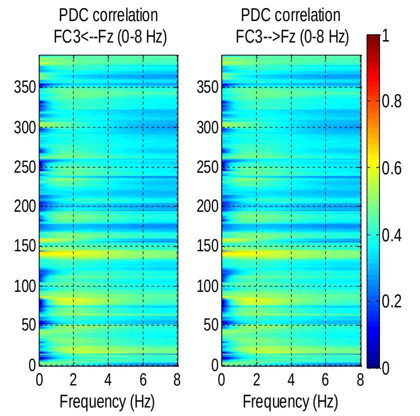

Fig. 3. b) PDC for movement recordings, FC3-Fz, 0-8 Hz (Rec011 DB1).

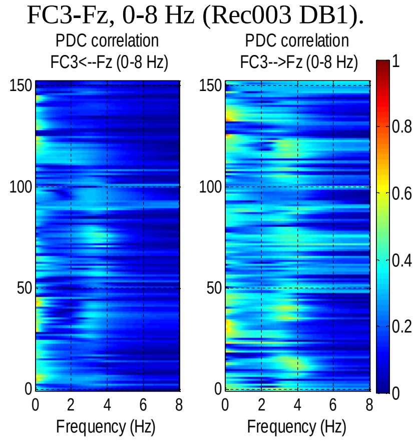

Fig. 3. c) PDC for motor imagery of the left hand, FC3-Fz, 0-8 Hz (Rec004 DB2).

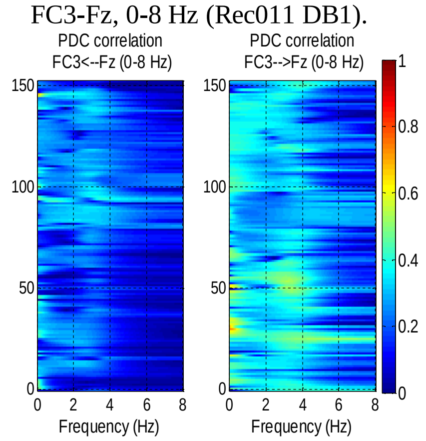

Fig. 3. d) PDC for motor imagery of the right hand, FC3-Fz, 0-8 Hz (Rec702 DB2).

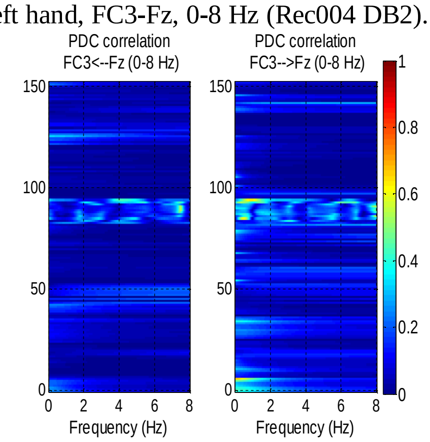

Fig. 3. e) PDC for rest recordings, FC3-Fz, 0-8 Hz (Rec014 DB2).

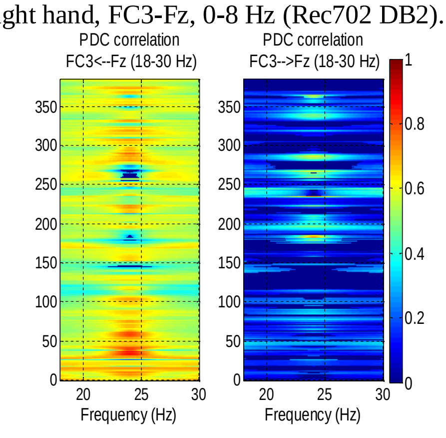

Fig. 3. f) PDC for motor imagery, FC3-Fz, 18-30 Hz (Rec003 DB1).

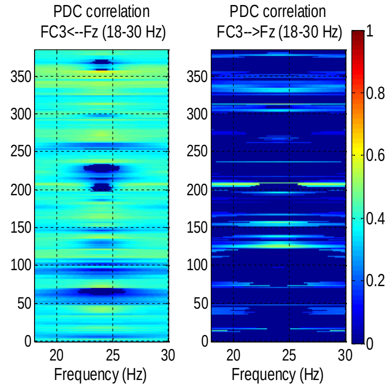

Fig. 3. g) PDC for movement recordings, FC3-Fz, 18-30 Hz (Rec011 DB1).

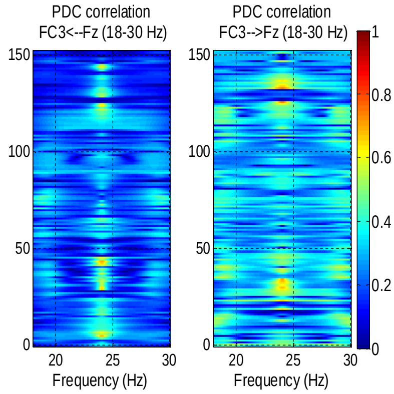

Fig. 3. h) PDC for motor imagery of the left hand, FC3-Fz, 18-30 Hz (Rec004 DB2).

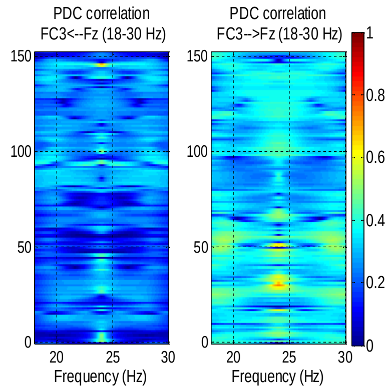

Fig. 3. i) PDC for motor imagery of the right hand, FC3-Fz, 18-30 Hz (Rec702 DB2).

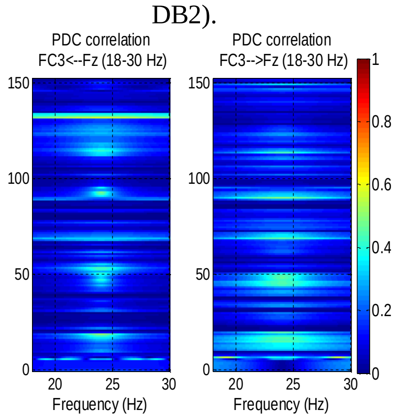

Fig. 3. j) PDC for rest recordings, FC3-Fz, 18-30 Hz (Rec014 DB2).

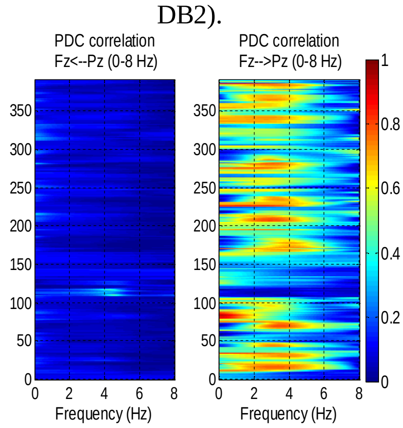

Fig.4. a) PDC for motor imagery, Fz-Pz, 0-8 Hz (Rec003 DB1).

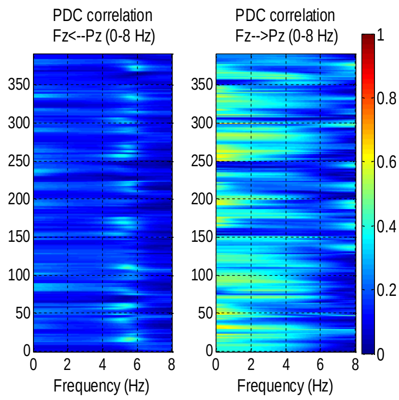

Fig. 4. b) PDC for movement recordings, Fz-Pz, 0-8 Hz (Rec011 DB1).

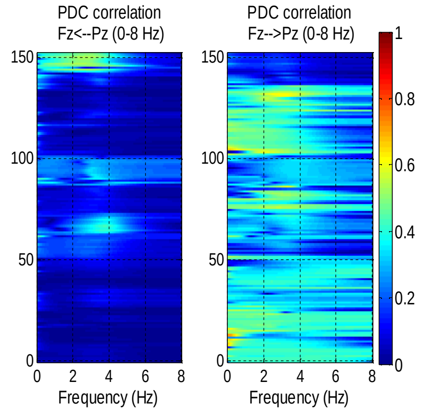

Fig. 4. c) PDC for motor imagery of the left hand, Fz-Pz, 0-8 Hz (Rec 004 DB2)

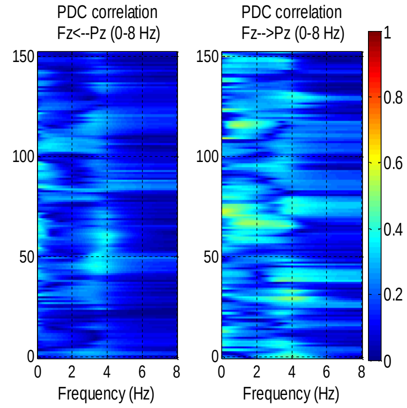

Fig. 4. d) PDC for motor imagery of the right hand, Fz-Pz, 0-8 Hz (Rec 702 DB2)

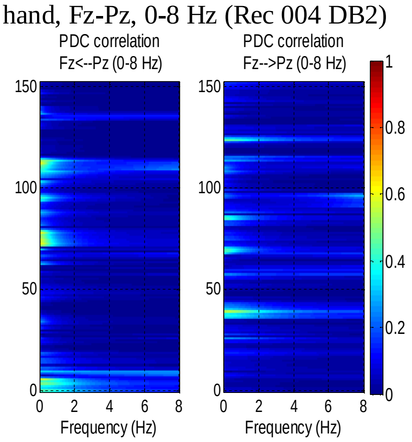

Fig. 4. e) PDC for rest recordings, Fz-Pz, 0-8 Hz (Rec014 DB2)

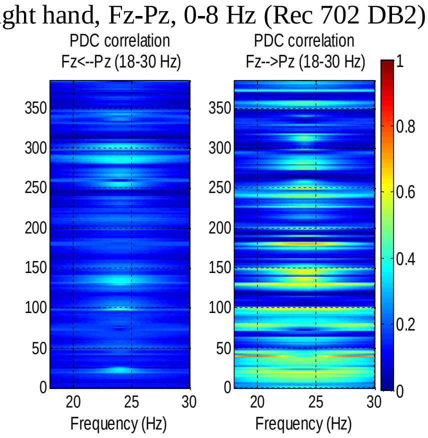

Fig. 4. f) PDC for motor imagery, Fz-Pz, 18-30 Hz (Rec003 DB1)

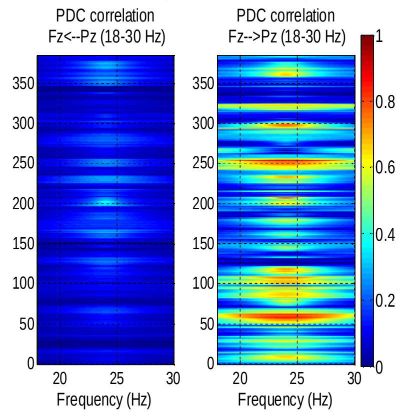

Fig. 4. g) PDC for movement recordings, Fz-Pz, 18-30 Hz (Rec011 DB1)

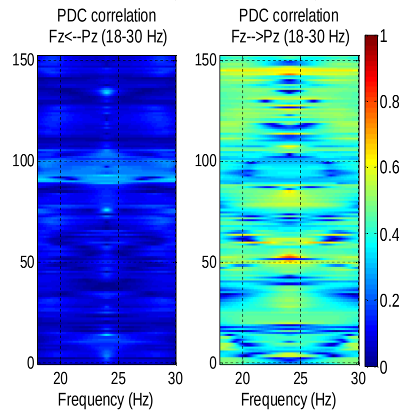

Fig. 4. h) PDC correlation for motor imagery of the left hand, Fz-Pz 18-30 Hz (Rec004 DB2)

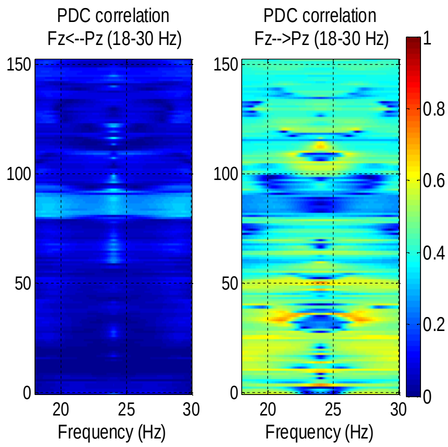

Fig. 4. i) PDC for motor imagery of the right hand, Fz-Pz, 18-30 Hz (Rec702 DB2).

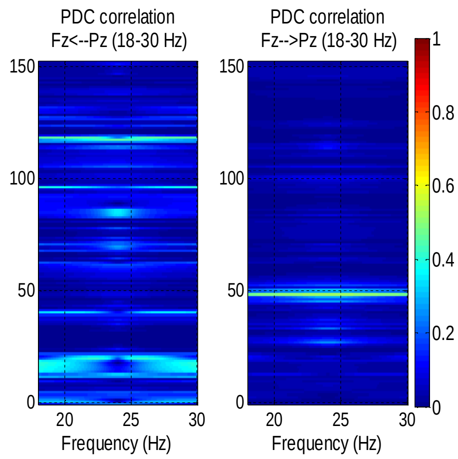

Fig. 4. j) PDC for rest recordings, Fz-Pz, 18-30 Hz (Rec014 DB2).

The PDC indicator value is determined by analysing the Hanning windowed signal. We obtain the heat map of values for channel pairs, both direct and indirect influences, when analysing the lowest frequency band between 0,...,8 Hz and the highest frequency band 18,...,30 Hz. These heat maps are presented in Figs. 2,...,4. The channel pairs chosen for this comparison are F1-F2, FC3-Fz and Fz-Pz, due to the fact that these pairs cover the majority of the brain areas analysed. These figures provide a visual comparison between different types of recordings at different frequencies. The heat map is a representation of PDC correlation value for a specific recording, given as example, determined for each Hanning windowed signal. The correlation parameter takes values between [0;1], as mentioned before, and as the reference scale in the presented figures suggests. We can observe similarities between motor imagery recordings from the two analysed databases, within the same frequency band.

The difference observed is between the frequency bands and between motor imagery recordings and rest or movement recordings. The heat maps presented for recordings taken as examples support the results presented in Tables 2,...,6, showing high PDC correlation values for the channel pairs presented. This indicates that the corresponding brain areas for these channel pairs, *i.e.* the central area represented by pair FC3-Fz (Fig. 3), the frontal area represented by pair F1-F2 (Fig. 2) and the link between the frontal and parietal area represented by pair Fz-Pz (Fig. 4) are all active during motor imagery tasks and deactivate during resting periods. The frequency bands analysed also influence the coupling level. This is to be expected given that the higher frequency band of 18,...,30 Hz corresponds to brain rhythm Beta2, specific for motor activities that are processed in the frontal lobe and integrated with sensory feedback in the parietal lobe. The central-parietal-occipital area of the brain is responsible for the multisensory integration (vision, hearing and somatic) predominant in the parietal region and the processing of spatial orientation in the posterior parietal lobe.

We also compute, for the same channel pairs and frequency bands mentioned before, (F1-F2, FC3-Fz and Fz-Pz) the 2D scatter of the PDC correlation indicator values in order to determine the degree of separability between recordings corresponding to motor imagery tasks and recordings of resting periods or movement. For the first database (DB1), given that there are no resting period recordings analysed, we simply present the values obtained for the correlation parameter for motor imagery and movement recordings (Fig. 5). After analysing DB2, we obtain the results presented in Fig. 6. These consist in the difference between values for motor imagery and resting period correlation of channel pairs. These show that the data can be clustered between certain intervals of the scale of [0;1].

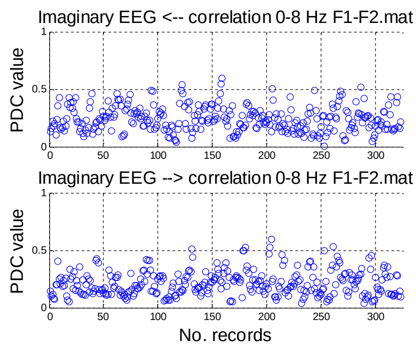

Fig. 5. a) Scatter of PDC values for motor imagery, F1-F2, 0-8Hz (DB 1).

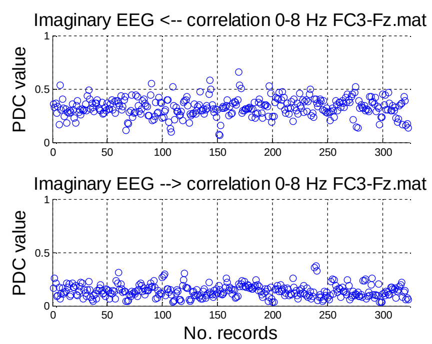

Fig. 5. b) Scatter of PDC values for motor imagery, FC3-Fz, 0-8Hz (DB 1).

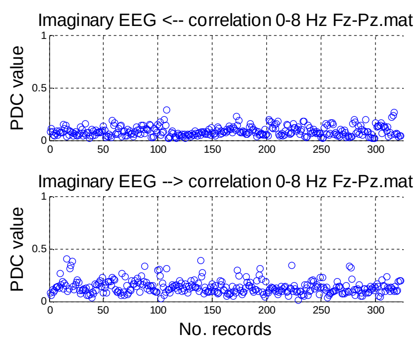

Fig. 5. c) Scatter of PDC values for motor imagery, Fz-Pz, 0-8Hz (DB 1).

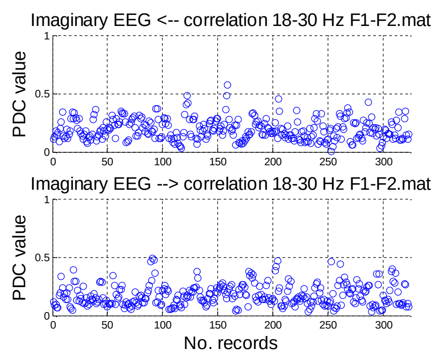

Fig. 5. d) Scatter of PDC values for motor imagery, F1-F2, 18-30Hz (DB 1).

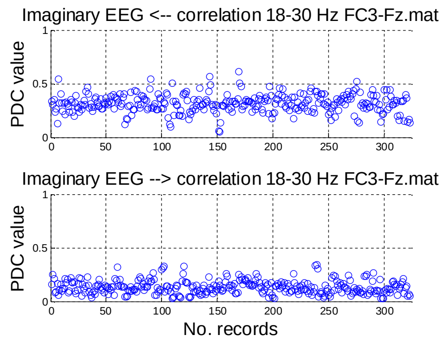

Fig. 5. e) Scatter of PDC values for motor imagery, FC3-Fz, 18-30Hz (DB 1).

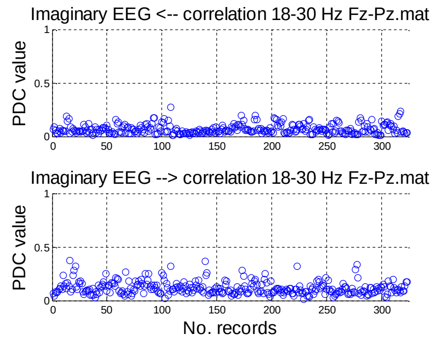

Fig. 5. f) Scatter of PDC values for motor imagery, Fz-Pz, 18-30Hz (DB 1).

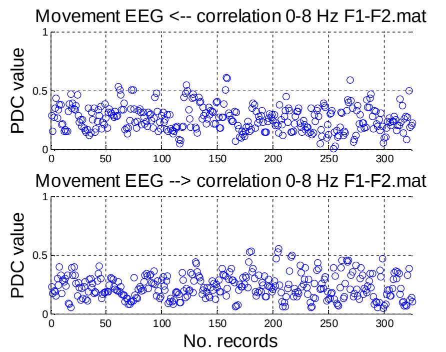

Fig. 5. g) Scatter of PDC values for movement recordings, F1-F2, 0-8Hz (DB 1).

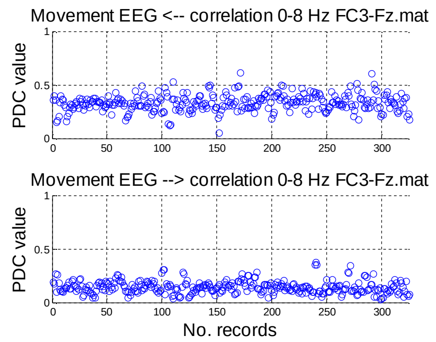

Fig. 5. h) Scatter of PDC values for movement recordings, FC3-Fz, 0-8Hz (DB 1).

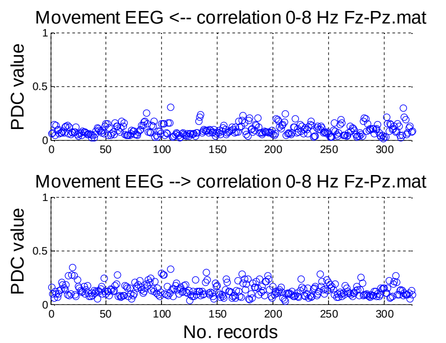

Fig. 5. i) Scatter of PDC values for movement recordings, Fz-Pz, 0-8Hz (DB 1).

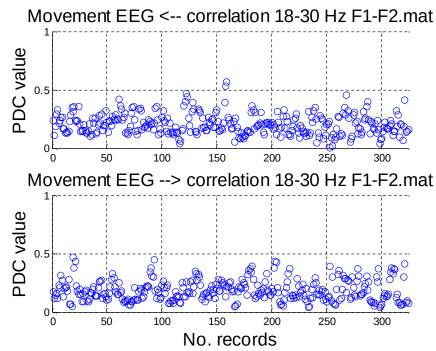

Fig. 5. j) Scatter of PDC values for movement recordings, F1-F2, 18-30Hz (DB 1).

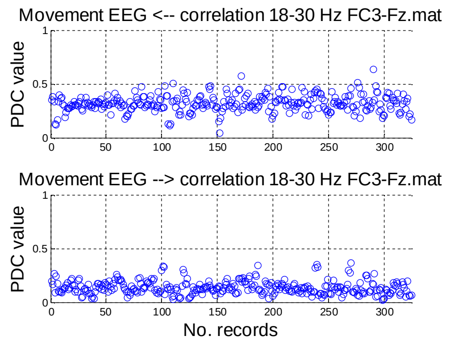

Fig. 5. k) Scatter of PDC values for movement recordings, FC3-Fz, 18-30Hz (DB 1).

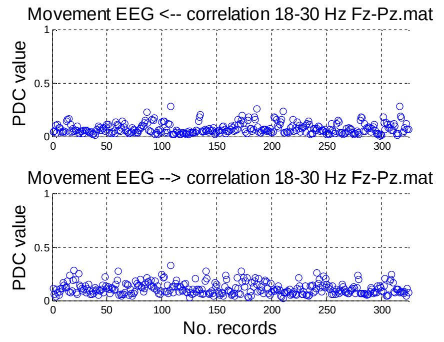

Fig. 5. l) Scatter of PDC values for movement recordings, Fz-Pz, 18-30Hz (DB 1).

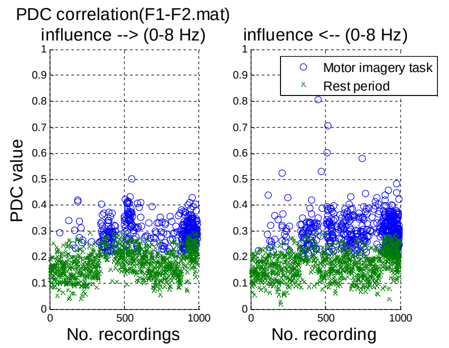

Fig. 6. a) 2D scatter of PDC values for left motor imagery, F1-F2, 0-8 Hz (DB2).

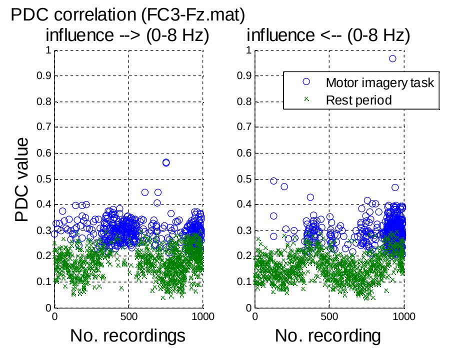

Fig. 6. b) 2D scatter of PDC values for left motor imagery, FC3-Fz, 0-8 Hz (DB2).

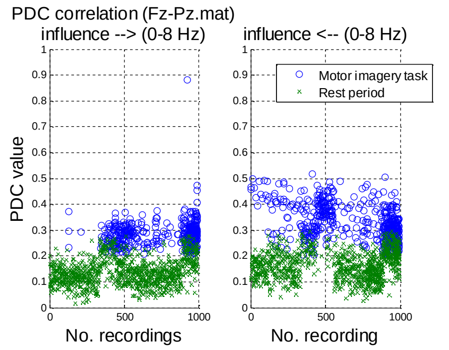

Fig. 6. c) 2D scatter of PDC values for left motor imagery, Fz-Pz, 0-8 Hz (DB2).

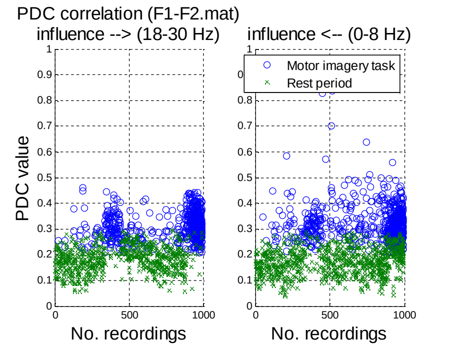

Fig. 6. d) 2D scatter of PDC values obtained for left motor imagery, F1-F2, 18-30 Hz (DB2).

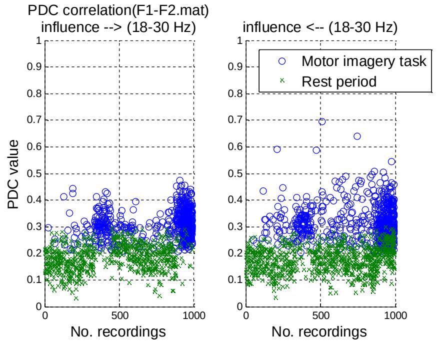

Fig. 6. e) 2D scatter of PDC values for left motor imagery, FC3-Fz, 18-30 Hz (DB2).

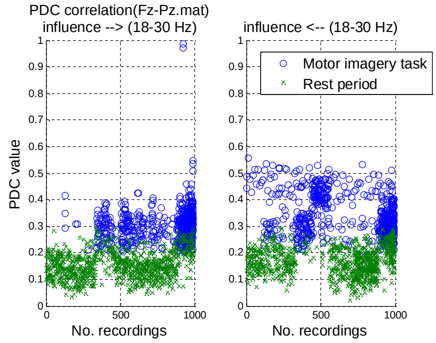

Fig. 6. f) 2D scatter of PDC parameter values for left motor imagery, Fz-Pz, 18-30 Hz (DB2).

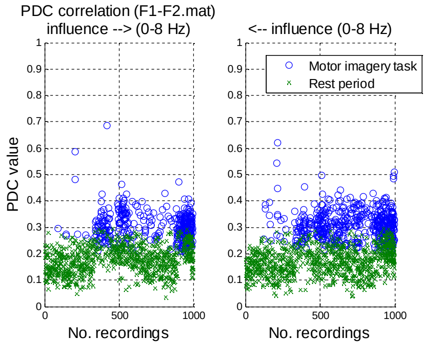

Fig. 6. g) 2D scatter of PDC values for right motor imagery, F1-F2, 0-8 Hz (DB2).

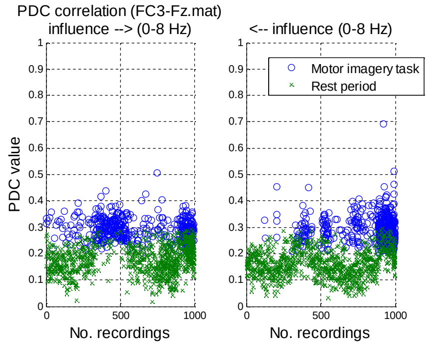

Fig. 6. h) 2D scatter of PDC values for right motor imagery, FC3-Fz, 0-8 Hz (DB2).

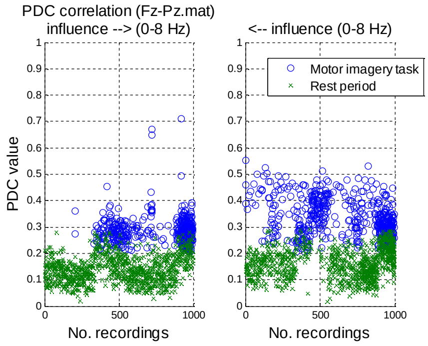

Fig. 6. i) 2D scatter of PDC values for right motor imagery, Fz-Pz, 0-8 Hz (DB2).

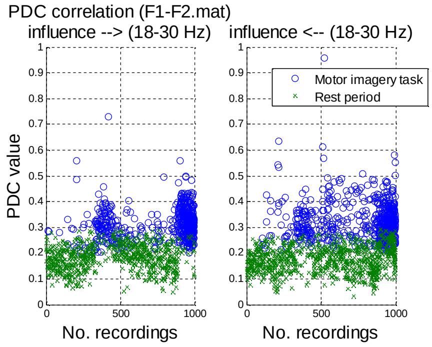

Fig. 6. j) 2D scatter of PDC values obtained for right motor imagery, F1-F2, 18-30 Hz (DB2).

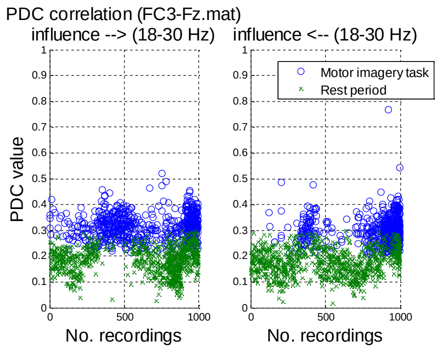

Fig. 6. k) 2D scatter of PDC values for right motor imagery, FC3-Fz, 18-30 Hz (DB2).

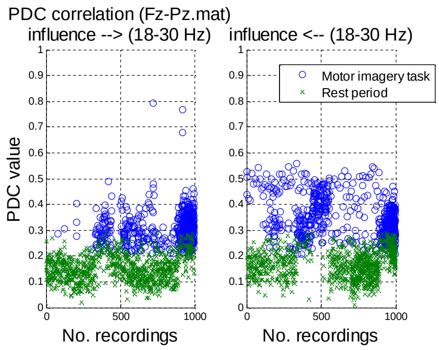

Fig. 6. l) 2D scatter of PDC values for right motor imagery, Fz-Pz, 18-30 Hz (DB2).

The results obtained for DB2 and presented in Fig. 6 are the most suggestive, as they show a clear separation of the recordings into two classes: motor imagery task recordings and rest period recordings. There is also a suggestive difference in terms of the analysis of frequency bands. The low frequency band 0,...,8 Hz presents a lower degree of correlation, whereas the high frequency band 18,..,30 Hz presents a higher degree of correlation, results also presented in Tables 2,...,6 in terms of mean values and standard deviation.

4. Conclusions

The comparison between the two analysed databases, DB1 and DB2, is necessary in order to determine differences between data acquisition in motor imagery practices. The results obtained show that recordings that contain only motor imagery tasks have a higher PDC correlation parameter value, compared to recordings that contain both motor imagery and resting periods. By dividing the EEG frequency domain into frequency bands based on the specific EEG rhythms also shows that high frequency components, 18,...,30 Hz, have a higher degree of coupling due to the fact that this frequency band corresponds to rhythms specific to motor imagery or movement recordings (Beta rhythm).

The correlation parameter obtained through the PDC method indicates high correlation between specific channel pairs. The analysis presented as a comparison between the two EEG databases indicates that multiple brain areas are active during motor imagery tasks, specifically the frontal area responsible for movement and the central-parietal-occipital area responsible with integrating data from sensory feedback (visual, audio or neuro-motor feedback). Both direct and indirect influence correlation for motor imagery tasks are indicators that there is constant feedback between brain areas and sensory components of the human body. We also have to take into account that we obtained high correlation values for channel pairs situated on different brain hemispheres, e.g. channel pairs FC3-Fz/FC4-Fz or C3-Pz/C4-Pz, meaning that both brain hemispheres are involved in motor imagery tasks. As a reference, we use the rest period recordings from DB2 that indicate low correlation between channel pairs due to low brain activity.

The implementation of a BCI system that uses a multichannel EEG configuration requires the identification and analysis of the most influential EEG channels. The PDC analysis is used to identify channels that are suitable for this application, in order to reduce the computational complexity of the BCI system and the corresponding algorithm.

Acknowledgment. This work was supported by a grant of the Romanian National Authority for Scientific Research and Innovation, CNCS – UEFISCDI, project number PN-II-RU-TE-2014-4-0832 "Medical signal processing methods based on compressed sensing; applications and their implementation".

REFERENCES

Adochiei F., Schultz S., Edu I., Costin H. and Voss A., *A New Normalised Short Time PDC for Dynamic Coupling Analyses*, Biomedical Engineering/ Biomedizinische Technik, **58**, 1 (2013a).

Adochiei F.C., Schultz S., Edu I.R., Costin H., Voss A., *A New Normalized Short Term PDC for Dynamic Coupling Analysis in Hypertensive Pregnant Women*, BMT, 2013b.

Baccala L.A., Sameshima K., *Partial Directed Coherence: a New Concept in Neural Structure Determination*, Byological Cybernetics, **84**, 463-474 (2001).

Baccala L.A., Sameshima K., Takahashi D.Y., *Generalized Partial Directed Coherence*, 15th Internat. Conf. on Digital Signal Processing, 163-166, 2007.

Blankertz B., Dornhege G., Krauledat M., Muller K.R., Curio G., *The Non-Invasive Berlin Brain-Computer Interface: Fast Acquisition of Effective Performance in Untrained Subjects*, J. of Neuroimage, **37**, *2*, 539-550 (2007).

Friston K., Moran R., Seth A.K., *Analysing Connectivity with Granger Causality and Dynamic Causal Modelling*, Current opinion in Nerubiology, **23**, *2*, 172-178 (2013).

Goldberger A.L., Amarai L.A.N., Glass L., Hausdorff J.M., Ivanov P.CH., Mark R.G., Mietus J.E., Moody G.B., Peng C.K., Stanley H.E., *Physiobank, PhysioToolkit and PhysioNet: Components of a New Research Resource for Complex Physiological Signals*, Circulation, **101**, *23*, e215-e220 (2000).

Lee K., Kim K., Song J., Ryu J., Kim Y., Park C., *Estimation of Brain Connectivity During Motor Imagery Tasks Using Noise-Assisted Multivariate Empirical Mode Decomposition*, J. of Electrical Engng. & Technol., **11**, *6*, 1812-1824 (2016).

Liang S., Choi K., Qin J., Wang Q., Pang W., Heng P., *Discrimination of Motor Imagery Tasks via Information Flow Pattern of Brain Connectivity*, Technology and Health Care, **24**, 795-801 (2016).

Niedermeyer E., *Chapter 9: The Normal EEG of the Waking Adult, Electroencephalography: Basic Principles, Clinical Applications and Related Fields*, 167-192, 2005.

Omidvarnia A., Azemi G., Boashash B., O'Toole J.M., Colditz P.B., Vanhatalo S., *Measuring Time-Varying Information Flow in Scalp EEG Signals: Orthogonalized Partial Directed Coherence*, IEEE Trans.s on Biomedical Engng., **61**, *3*, 680-693 (2014).

Petti M., Toppi J., Babiloni F., Cincotti F., Mattia D., Astolfi L., *EEG Resting-State Brain Topological Reorganization as Function of Age*, J. of Computational Jntelligence and Neuroscience, **2016**, Art. ID 6243694, 1-11 (2016).

Pfurtscheller G., Neuper C., Guger C., Harkman W., Ramoser H., Schlogl A., Obermaier B., Pregenzer M., *Current Trends in Brain-Computer Interface (BCI) Research*, IEEE Trans. on Rehabilitation Engng., **8**, *2* (2000).

Pichiorri F., Morone G., Petti M., Toppi J., Pisotta I., Molinari M., Mattia D., *Brain-Computer Interface Boosts Motor Imagery Practice During Stroke Recovery*, Annals of Nuerology, **77**, *5*, 851-865 (2015).

Podder P., Khan T.Z., Khan M.H., Rahman M.M., *Comparative Performance Analysis of Hamming, Hanning and Blackman Window*, Internat. J. of Computer Appl., **96**, *18* (2014).

Samdin S.B., Ting C.M., Salleh S., Hamedi M., Mohd Noor A.B., *Estimating Dynamic Cortical Connectivity from Motor Imagery EEG Using Kalman Smoother and EM Algorithm*, IEEE Workshop on Statistical Signal Processing (SPP), 181-184, 2014.

Shalk G., McFarland D.J., Hinterberger T., Wolpaw J.R., *BCI2000: a General Purpose Brain-Computer Interface (BCI) System*, IEEE Trans. on Biomedical Engng., **51**, *6*, 1034-1043 (2004).

Tsoneva T., Baldo D., Lema V., Garcia-Molina G., *EEG-Rhythm During a 2back Working Memory Task and Performance*, IEEE Ann. Internat. Conf. of Engng. in Medicine and Biology Soc., 3828-3831, 2011.

Xu H., Lou J., Su R., Zhang E., *Feature Extraction and Classification of EEG for Imaging Left-Right Hands Movement*, 2nd IEEE Internat. Conf. on Computer Sci. a. Inform. Technol. (ICCSIT), 56-59, 2009.

* * * Link 1 - http://www.schalklab.org/research/bci2000.

* * * Link 2 - http://www.bbci.de/competition/iv/#dataset1.

STUDIUL CUPLĂRII CANALELOR ELECTROENCEFALOGRAFICE ÎN ANALIZA MULTIPLELOR BAZE DE DATE

(Rezumat)

Analiza semnalelor Electroencefalografice (EEG) pentru activități motor-imaginare se utilizează pentru a implementa aplicații de interfațare om-calculator. Acest aspect implică înțelegerea semnalelor cerebrale în timpul activităților motor-imaginare. Utilizarea metodei coerenței parțiale directe (partial directed coherence – PDC) pentru analizarea multiplelor baze de date de semnale EEG poate determina nivelul de cuplare dintre canale pentru a identifica modul de procesare şi achiziția de date EEG în aplicații de interfațare om-calculator. Acest lucru este necesar pentru a reduce timpul de procesare şi timpul de răspuns al unor sisteme dezvoltate pentru interacționarea dintre om şi calculator.